ELSEVIER

Applied Surface Science 89 (1995) 175–185

applied surface science

The (0001)-surface of 6H-SiC: morphology, composition and structure

U. Starke *, Ch. Bram, P.-R. Steiner, W. Hartner, L. Hammer, K. Heinz, K. Müller

Lehrstuhl für Festkörperphysik, Universität Erlangen-Nürnberg, Staudtstrasse 7, D-91058 Erlangen, Germany

Received 22 august 1994; accepted for publication 31 January 1995

Abstract

The morphology, composition and structure of wet chemically prepared 6H-SiC(0001) samples were investigated immediately after introduction into vacuum. Scanning tunneling microscopy displayed large atomically flat areas on the surface. The step structure found is correlated to the sample periodicity normal to the surface. Most step heights are multiples of half the vertical unit cell length. Low-energy electron diffraction (LEED) revealed good surface order with bulk-like lateral periodicity. From high-resolution electron energy loss spectroscopy the saturation of dangling bonds with hydroxyl species could be determined. This termination is responsible for an electron beam sensitivity found in LEED. Upon annealing the oxygen is removed and carbon–carbon bonds develop on the surface as demonstrated by Auger electron spectroscopy. This new structure is ordered in a $(\sqrt{3} \times \sqrt{3})R30°$ periodicity.

1. Introduction

Silicon carbide is a material expected to fill recess areas of electronic device applications where substrate materials as Si, Ge or III–V and II–VI compounds cannot provide suitable electronic parameters [1]. The unique properties of SiC, like high-temperature stability and thermal conductivity, fast free carrier recombination and large band gap, provide the grounds for present and future development of fast, high-power and high-temperature devices. Typical examples are the high-temperature MOS-FET [2] or the blue LED [3]. SiC can crystallize in a variety of allotropes (polytypism [4]). With respect to structure, the difference between different polytypes can be expressed as a variation of the stacking sequence of hexagonal bilayers in a hexagonal lattice; and polytypes with unit cell lengths of several 100 Å along the *c*-axis have been found. The (bilayer) stacking sequence would be ABCABC for the zinc blende (3C-SiC), ABABAB for the wurtzite (2H-SiC), ABCBA for the 4H-SiC, and ABCACBA for the 6H-SiC structure. Details of the stacking structure of polytypes are discussed elsewhere [5]. The important electronic accompaniment of this allotropy is the large spread in band-gap energies between different polytypes. Zinc blende and wurtzite structures are the extreme cases with experimentally obtained excitonic energy gaps (extrapolated to 0 K) of 2.39 and 3.33 eV, respectively [6]. In combination, the presence of polytypism for silicon carbide might eventually allow the development of sandwich devices with layers having different electronic properties without structural lattice mismatch.

* Corresponding author. Corresponding author. Tel.: +49 9131 858405; Fax: +49 9131 858400; E-mail: ustarke@erympel.rrze.uni-erlangen.de.

SSDI 0169-4332(95)00024-0

Despite these valuable properties and promising perspectives the growth of well-ordered crystalline SiC of low defect density is not yet easily controlled and still is a current research topic. The growth of bulk-like material is routinely possible, e.g., using the Acheson [7] or Lely process [8,9], and polytypes may be produced as desired. However, this type of material exhibits an enormous density of structural defects ($\sim 10^{17}$ cm^{-3}) and is not suitable for electronic devices [1]. Only epitaxially grown material seems to provide the electronic properties necessary for the development of new devices to fill the above-mentioned technological niches.

The growth process of epitaxial SiC layers on Si substrates, especially Si(100), was extensively investigated by Powell's group. It was found that the considerable lattice mismatch between Si and SiC induces strain and structural defects in the SiC film [10,11]. The introduction of buffer layers can reduce this problem [12]. Still, high-temperature applications are restricted, and only β-SiC can be grown by this technique. Alternatively, SiC films may be grown homoepitaxially on bulk SiC material. Naturally, SiC grows along the *c*-axis exhibiting its hexagonal planes. Powell et al. could obtain a cubic SiC film on an unpolished substrate of the Lely type [13]. Other polytypes, e.g. 6H, can be obtained when substrate material of the same kind is cut and polished slightly off-normal (e.g., 5° off the *c*-axis) [14,15], obviously by influence of the step structure. In a different investigation 6H-material has also been produced on planar 6H-substrates [16], and it was proposed that seeds of cubic material develop from substrate defects while on flat surface areas the substrate polytype is continued. Still on an atomic scale, even a flat surface exhibits enough steps to provide sufficient correlation to the substrate structure, and above arguments may not be contradicting. In this respect, microscopic understanding of the growth process is still missing. The atomic structure of surface and interface has to be resolved in order to understand the epitaxial growth mechanism and eventually predict appropriate conditions to obtain a certain crystallographic allotrope.

A variety of surface studies of single crystalline SiC have been published. However, most of these studies deal with the (100) surface of cubic material. Only a few groups have concentrated on the basal plane of cubic or hexagonal material [17–30], and in all cases the samples were subjected to in-situ preparation either by thermal treatment, exposure to Si flux or oxidation procedures. Ordered surfaces were observed only after such treatment. Superstructures with large surface unit cells were reported early [17]. Later it was found that superstructures are present on carbon- or silicon-rich surfaces, while surfaces with bulk-like stoichiometry could not be reproducibly prepared [25].

In an industrial growth process extensive preparation in vacuum is not possible. Surfaces are rather prepared by chemical procedures alone. Of course, further surface modifications happen during the deposition process or under exposure of reactive gases. To provide insight in the crystal properties in the initial stage, the present paper reports about the structure of SiC surfaces obtained by a chemical preparation immediately followed by transfer into vacuum. After a brief description of experiment and chemical sample treatment the morphology and composition of the surface are presented as it is obtained from scanning tunneling microscopy (STM) and Auger electron spectroscopy (AES). The ensuing sections describe the atomic surface structure with respect to bulk geometry and dangling-bond termination by means of low-energy electron diffraction (LEED) and high-resolution electron energy loss spectroscopy (HREELS). Finally, surface modifications upon thermal treatment are demonstrated in the light of LEED and AES measurements.

2. Experiment

In the present experiments homoepitaxially grown 6H-SiC film samples were used. The substrate material was bulk SiC grown by a modified Lely process [9]. The epilayers were generated by chemical vapor deposition (CVD) [31]. The samples used in this work (four altogether) were provided by Siemens AG (Erlangen) and Professor R. Helbig (Angewandte Physik, University of Erlangen-Nürnberg). All samples were nominal (0001)-oriented, i.e., silicon-terminated, although this was not checked by crystallographic methods. As judged from the preparation procedure they were assumed to be n-type with a donor concentration in the 10^{17} cm^{-3} range.

From different CVD runs samples with different dopant concentrations were obtained. Corresponding effects on the surface properties could not be observed. Only a very low conducting sample presented charging problems in LEED at energies below 90 eV.

From initial tests it turned out that by simply etching the samples in hydrofluoric acid and subsequent preparation in vacuum, atomically flat and well-ordered surfaces could not be obtained. This was confirmed for several samples and different polytypes. In this status of sample preparation the outermost sample part is obviously crystallographically rough, possibly from the CVD switch-off or from an optional polishing procedure. Conventional UHV procedures are not successful to remove the disordered part from the surface. However, a special ex-situ preparation by a combined oxidation and etching process uncovered a crystalline surface of the film, as apparent from sharp LEED patterns, described in detail in Section 3.3. In the present work oxidation was carried out in a furnace by heating the sample to 800° C under 1 bar O_2 for about 4 hours. Afterwards, the sample was cleaned with aqua regia, rinsed in acetone and subsequently etched in hydrofluoric acid (50%) and in buffered NH_4F (pH 8.7) to remove the oxide film. After a final rinsing in deionized water the sample was introduced into vacuum. The coarse scale morphology changes between these steps are depicted in Fig. 1 by scanning electron microscopy (SEM) images from a typical sample: in the initial stage a rich structuring of the surface is visible. The important point is that after oxidation the surface is basically flat with small patch structures present that are largely removed after the HF etching step. This is proven by Fig. 1c and holds at least for the scale displayed.

The surface analytical experiments were carried out in a twin UHV chamber with sample introduction and transfer facility. The main chamber was equipped with a four-grid reverse LEED optic for LEED and AES measurements. Due to the STM instrumental design [32] an auxiliary chamber part was attached for the STM measurements. The samples could be transferred in UHV between the two stages, and were introduced into vacuum immediately after chemical preparation with the same transfer system. For fresh samples no further treatment was applied before starting the UHV experiments. The HREELS experiments were carried out in a separate chamber. Here, the samples had to be

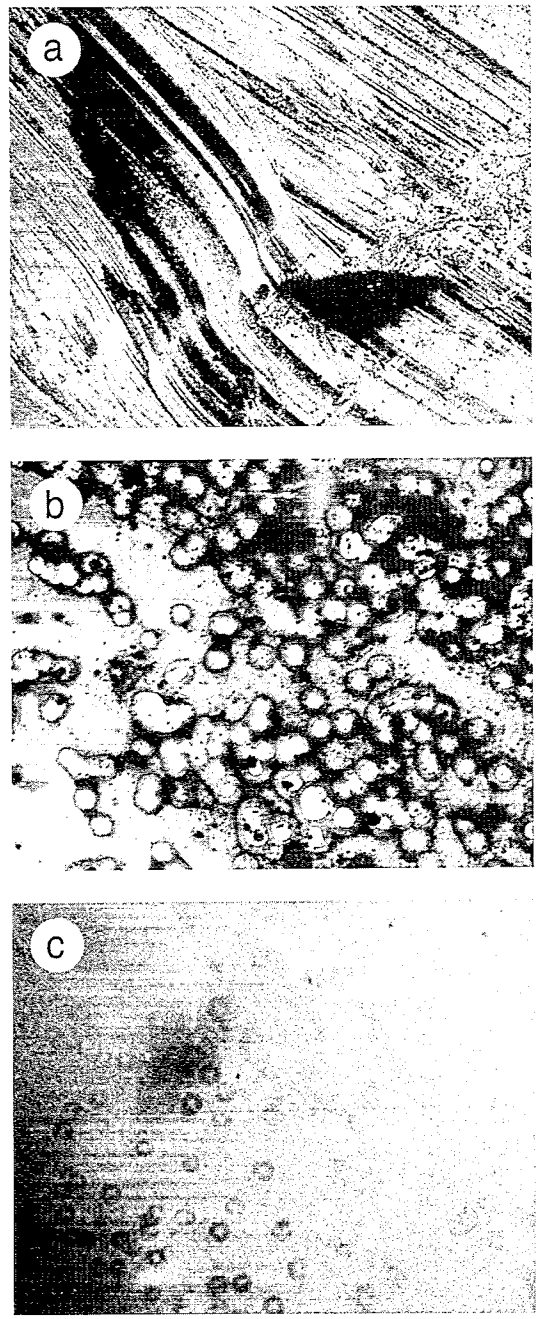

Fig. 1. SEM images of a 6H-SiC(0001) sample. A 530×530 μm^2 area is shown (a) before chemical treatment, (b) after oxidation in a furnace (800° C, 1 bar O_2, 4 hours), (c) after etching with HF (50%).

a

b

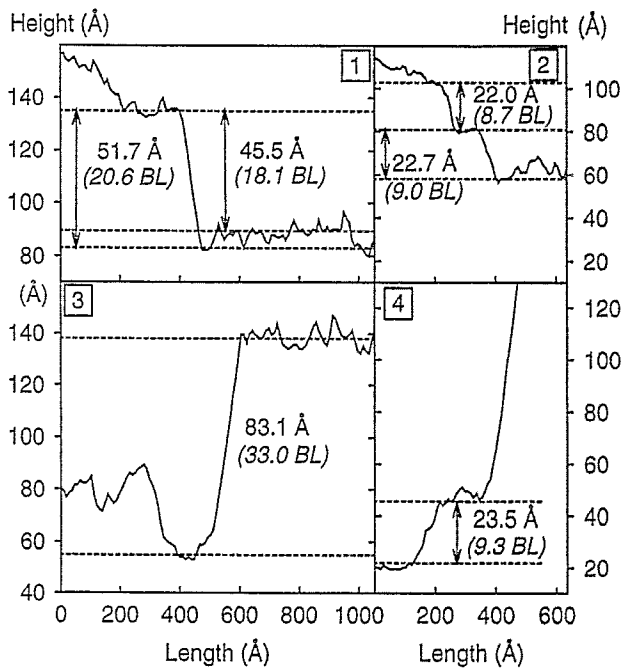

BL = bilayer height = 2.52 Å

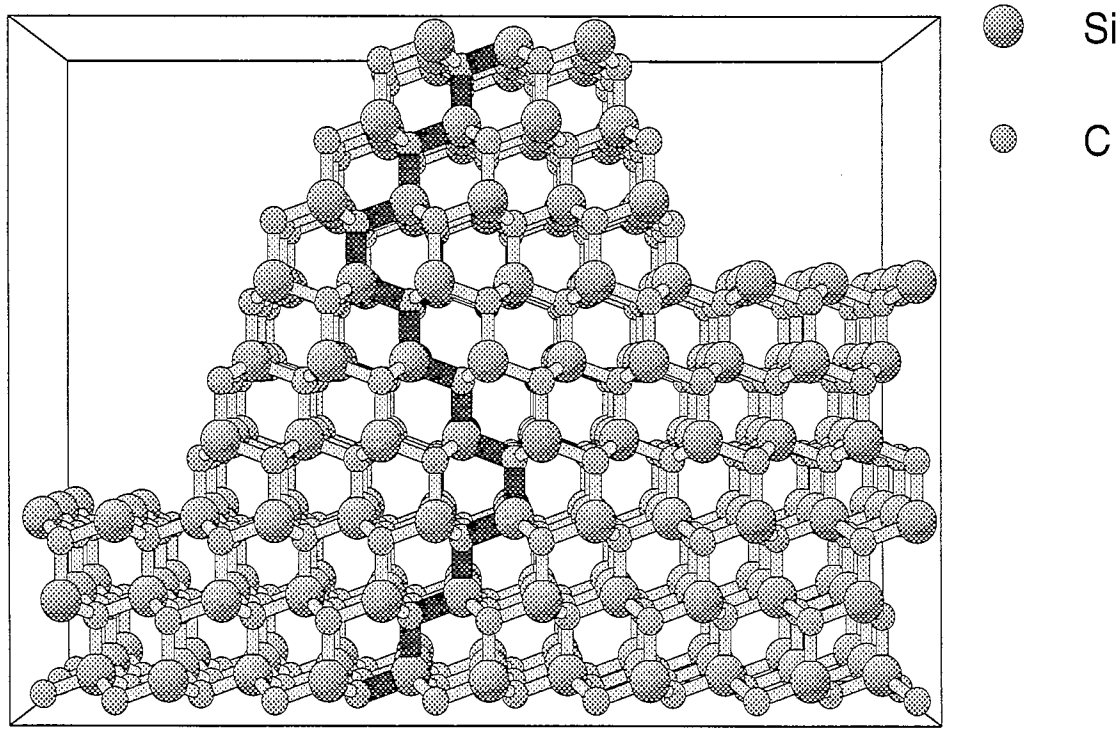

Fig. 3. Side view in [11$\bar{2}$0]-direction of the 6H-SiC(0001) surface with steps of three and six bilayer spacings.

mounted on a dedicated sample holder, thus breaking the vacuum. In order to check for a possible influence of the subsequent chamber bake-out, sample conditions were compared by means of LEED and AES, and no differences were observed.

3. Results

3.1. Morphology

The sample morphology after chemical treatment was monitored by STM. It turned out that, whether in air or in UHV, after this preparation stable tunneling conditions could only be obtained at large bias voltages (2.5 V and more) and in particular only for tunneling from filled states of the surface into the tip. Obviously dangling-bond orbitals are completely filled after the initial preparation procedure and no surface states are present within the energy gap. This could be due to some kind of atomic or molecular termination of these bonds as result of the etching process or of the final rinsing treatment. Possibilities to be considered in that respect include development of a surface oxide, hydrogen, or hydrocarbon termination, surface hydrides, or termination with hydroxyl groups, as discussed later in this paper in more detail. Due to the difficult tunneling conditions atomic resolution could not be achieved. In addition, water contamination is unavoidable for ex-situ prepared samples in the initial preparation status. Now, due to the saturation of dangling bonds the surface morphology contributes only a low tunneling current while diffusing water molecules can appear in the tunneling gap area and induce a large signal. Correspondingly, the STM images imply a disordered

Fig. 2. Morphology of a 6H-SiC(0001) sample immediately after preparation. (a) 5000 × 5000 Å STM image (2.91 V tip bias, 0.5 nA tip current) in topographic mode shows large (~ 1000 Å wide) atomically flat areas interrupted by up to 100 Å deep trenches. (b) Line scans show step heights of multiples of three bilayer spacings ($n \times 3 \times 2.52$ Å)

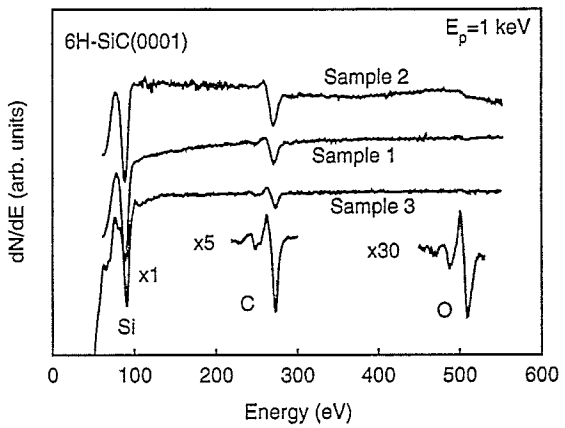

Fig. 4. Differential AES spectra of three 6H-SiC(0001) samples after chemical preparation (primary energy 1 keV). Insets show details of the carbon and oxygen peaks of sample 3.

surface with a considerable amount of particles distributed over the scanning area although this is not caused by the morphology as pointed out. Nevertheless, STM images could be successfully obtained in the topographic mode at a positive tip bias of ~ 2.9 V, typically, and tunneling currents in the 0.3 nA range. A SiC sample prepared according to the above recipe develops large atomically flat surface areas on a typical 1000 Å scale (cf., Fig. 2a). Trenches up to 100 Å deep can be observed that may be residually due to the surface morphology prior to the chemical preparation. The surface morphology of a 6H-sample (sample 4), as shown in Fig. 2a, was analyzed. Along the scanning direction it is possible to coarsely analyze the step structure of this sample. For four positions where the image noise is particularly low this is displayed by line scans in Fig. 2b. Step heights are determined by the difference between marks put at the step edges. The positioning of the marks was done before the grey scale was rescaled into Å in order to avoid any subjective influence. The tilt of the surface in this specific image is negligible for the evaluation of step heights. The line scans show a wide range of step heights present on the surface, as large as several tens of Å. A single bilayer step would be 2.52 Å high. A rescaling of the step structure in bilayer units depicts that the step heights are multiples of three bilayer distances. The frequent occurrence and accuracy of $3 \times n$ bilayer step heights rule out any influence of the noise level. Additionally, on another sample a large number of line scans was inspected with a Fourier analysis. Clear peaks were found for 3 and 6 bilayer step heigths. In view of the stacking sequence of the present 6H-polytype this suggests that the etching procedure predominantly exposes one of the three

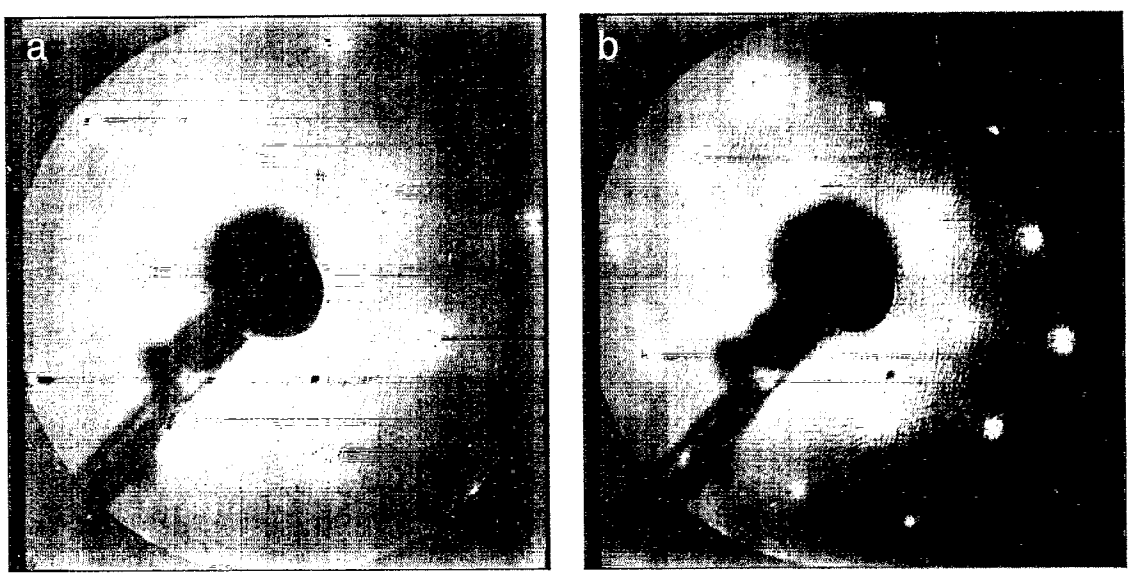

Fig. 5. LEED patterns of a 6H-SiC(0001) sample after chemical preparation showing bulk-like periodicity at energies of 97 eV (a) and 182 eV (b); angle of incidence not aligned.

inequivalent hexagonal layers. From STM we have no indication which layer this is. However, a LEED structure analysis that is being published elsewhere determines that the preferential stacking termination is ABCACBA [5]. The corresponding situation is sketched in Fig. 3 for a mono and a double step of triple bilayer height.

3.2. Carbidic surface

The chemical composition of a bulk-truncated surface is $Si_{0.5}C_{0.5}$. To monitor the composition as obtained after the chemical treatment AES was used. The acquisition of AES spectra and the evaluation of peak-to-peak ratios of the silicon and carbon transition is fairly straightforward, and several groups have used AES to investigate relative changes of the surface stoichiometry upon thermal or oxidation treatment [17,23–27,33–36], or upon Si evaporation [25]. However, it is difficult to obtain quantitative values of the composition due to a number of factors, e.g., electron mean free path and Auger transition matrix element or detector efficiencies, unless a gauge point with known structure and composition is available. As this was not true for the present case, the analysis was restricted to relative composition. An additional complication is the unknown quantity of contamination due to the mere chemical preparation. Water, hydrocarbons or even dust particles may be residual on the surface, obstructing the sample composition data, although a sharp LEED pattern is observed. Fig. 4 shows AES data from three different samples of nominally identical surface preparation. As was to be expected from the above arguments, the Si/C peak-to-peak ratio varies considerably in the range 2–5. This demonstrates the difficulty of stoichiometry determination of exclusively chemically prepared surfaces. However, the resolution of the spectra is sufficient to determine the carbidic nature of the surface carbon and the presence of oxygen in all three samples, as depicted for sample 3 by the inset in Fig. 4.

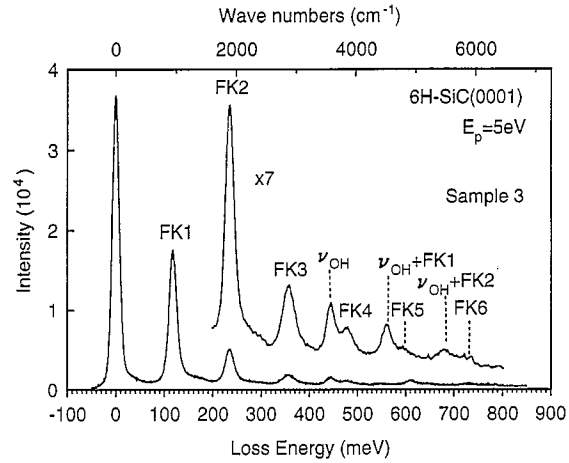

Fig. 7. Vibrational spectrum of a chemically prepared 6H-SiC(0001) sample by HREELS. Single and multiple excitation losses of the optical surface phonon ("Fuchs–Kliewer phonon") are indicated FKn. The peak at 443 meV, indicated ν_{OH}, is interpreted as the O–H stretching mode of hydroxyl species present on the surface. Combination losses are present in the spectrum (e.g., ν_{OH} + FK1).

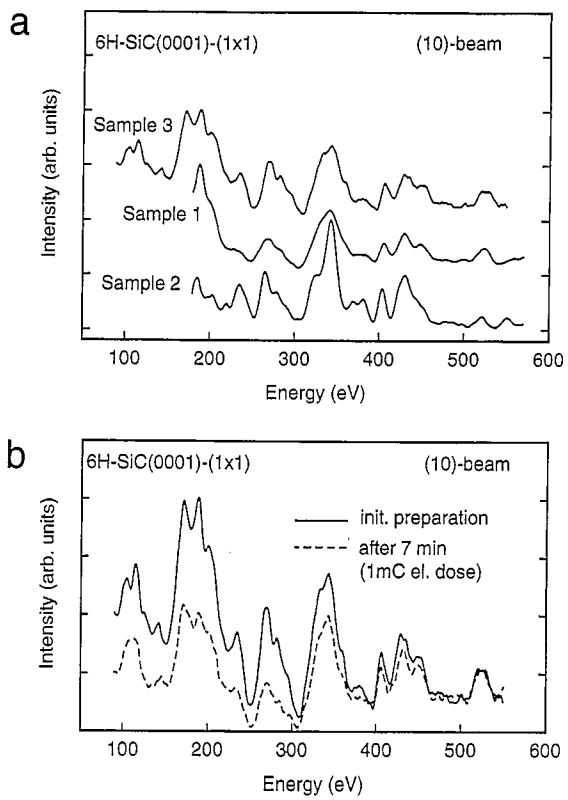

Fig. 6. LEED $I(E)$-spectra of the (10)-spot of (1×1)-6H-SiC(0001) averaged over symmetry equivalent beams in normal incidence conditions. (a) For three different samples after introduction in vacuum, (b) for sample 3 initially after chemical preparation (solid curve) and after prolonged electron irradiation (dashed line).

3.3. Surface structure

The chemical preparation recipe generates well-ordered surfaces with bulk periodicity. Fig. 5 shows respective LEED patterns with low background and spot distances corresponding to a (1×1) reciprocal unit cell with the bulk-like lattice constant of 2.04 $Å^{-1}$. In Fig. 6a the intensity of the (10)-spot as a function of electron energy ($I(E)$-spectra) is shown for the three samples 1–3 (cf., Fig. 4). The degree of reproducibility of the surface preparation can be depicted from this graph. Samples 2 and 3 display similar spectra as a fingerprint of identical surface structures, while the intensity curve for sample 1 is less structured. This smoother spectrum is indicative for a structural mixture present on the surface. The full sets of $I(E)$-data for the samples 1 and 2 were used for a detailed LEED structure analysis by which this difference could be verified [5].

The spot intensities decreased considerably during the LEED experiment (while the background increases). However, this effect was restricted to the electron impact position, and moving the sample restored the initial LEED pattern and intensities. That means that the electron beam causes a loss of order on the surface. The effect is demonstrated for one sample (#3) in Fig. 6b, where the (10)-spot $I(E)$-spectra of the initial situation are compared with dose after 7 min electron irradiation, corresponding to a dose of $\sim 10^{-3}$ C ($\sim$ 1000 electrons per unit cell). Both spectra are normalized to the primary beam current in order to provide an absolute comparison of the surface reflectivity. Clearly, the structure of the $I(E)$-spectra is identical; only an energy-dependent loss is noticeable that is mainly restricted to the energy range below 400 eV. This shows that the damage is concentrated in the immediate surface region. Possible reasons for the electron beam sensitivity may be the sample termination with an electron beam sensitive species or a charge-induced destruction of the sample surface. Unfortunately it was not possible to monitor the damage by AES due to the intense primary beam current necessary. At least no spectral changes with time were observed. Either the damage occurs too fast, or the composition of the surface is not altered.

Vibrational spectroscopy was applied in order to obtain some insight in the damage process through information about possible bond-saturating species. The HREEL spectrum for the SiC surface is dominated by single and multiple excitation losses of the optical surface phonon in the compound crystal – often called Fuchs–Kliewer-phonon (FK) in recognition of their detailed theoretical description [37]. These modes are an order of magnitude larger in intensity than molecular modes. Experimentally, one observes a reduced energy resolution, probably due to intra-conduction band transitions similar to pure silicon [38]. Unfortunately, this effect can only be limited by reducing the sample conductivity. As a necessary compromise a finite peak width has to be accepted, e.g. about 17 meV, as shown in Fig. 7 for sample 3. This finite peak width and the presence of

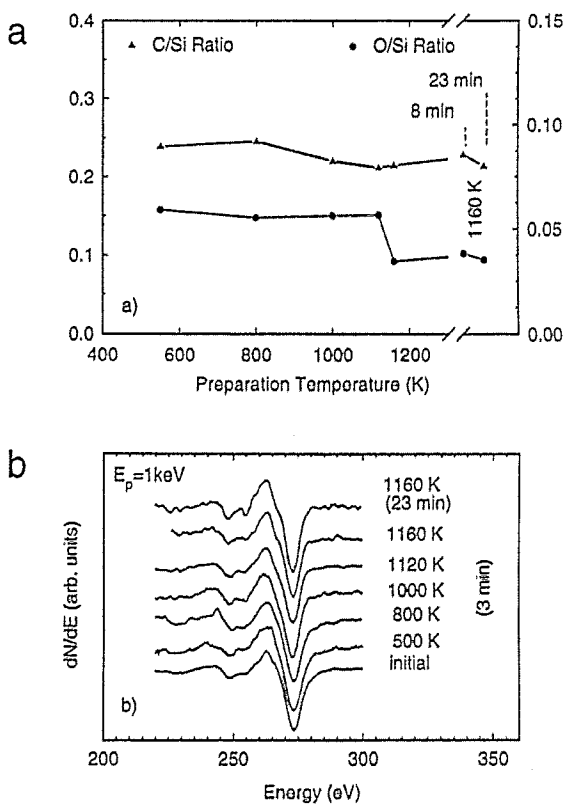

Fig. 8. Thermal treatment of 6H-SiC(0001) by annealing to different temperatures for 3 min, and longer heating times at 1160 K. The total time per temperature point is indicated. All measurements carried out at RT: (a) AES peak-to-peak ratios C/Si and O/Si for the fresh surface and as function of annealing temperature. Additional measurement points at 1160 K shown above the horizontal axis break. (b) AES carbon peak shape for different annealing steps (E_P = 1 keV).

multiple FK-losses obstruct important areas of the spectrum and complicate the interpretation of the data. However, it is still possible to identify a specific loss feature at 443 meV. Multiple combinations of this loss feature with FK-excitations are also present as expected. A detailed analysis of this spectrum and the changes upon electron dosage and thermal treatment strongly suggests that the loss represents hydroxyl species on the surface [39]. For comparison, on Si(100) the O–H stretching frequency was observed at about 460 meV [40]. Of course, it is not possible to completely exclude the presence of atomic hydrogen on the surface because the H–Si stretching vibration (~ 260 meV) is obstructed by the second FK-peak. Additionally, the detailed analysis also depicts a background of hydrocarbon-related losses that overlap with the FK triple loss. Respective combination losses (CH_x-FK1) can also influence and shift the OH feature. In summary, the vibrational analysis depicts OH species as pre-

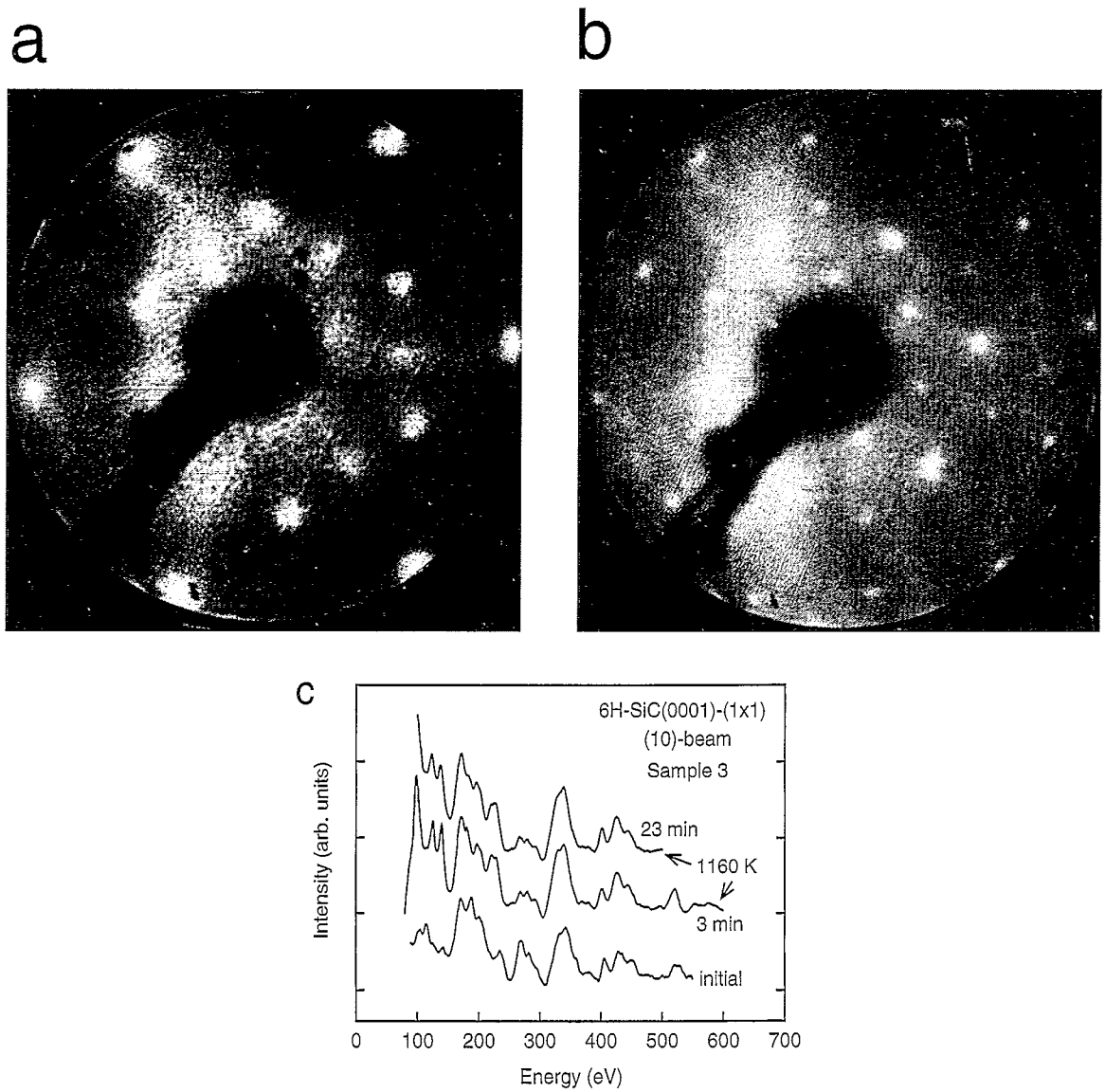

Fig. 9. SiC(0001)-($\sqrt{3} \times \sqrt{3}$)-R30° structure: (a) LEED pattern at $E_P = 49$ eV and (b) 115 eV, (c) $I(E)$-spectrum of (10)-beam for the initially prepared (1×1)-surface and after short and long annealing to 1160 K.

dominant bond saturation on the surface. Additionally, a non-uniformity of the molecular surface termination is indicated, as to be expected just after a chemical preparation.

3.4. Thermal treatment

The surface order can be restored by annealing to ~ 1100 K. The LEED pattern again displays (1 × 1) bulk-like periodicity. The surface composition as monitored by AES peak-to-peak ratios remained the same with respect to carbon and silicon. However, the oxygen signal was considerably reduced after heating to 1120 K, as shown in Fig. 8a. In some experiments oxygen was no longer detectable. The oxygen depletion coincided with a change of the carbon peak shape. While still clearly of carbidic form up to annealing temperatures of about 1000 K, the AES peak developed a low-energy shoulder above 1100 K that is typical for graphitic carbon chemistry (cf., Fig. 8b). The shoulder appeared more pronounced after extensive heating to about 1160 K, when also extra spots of a $(\sqrt{3} \times \sqrt{3})$R30° superstructure were visible in the LEED pattern (cf., Figs. 9a and 9b). These findings are in agreement with previous studies, e.g. by Kaplan [25], and suggest the development of carbon–carbon bonds after Si desorption. Note that this structural change should be accompanied by a stoichiometry change. However, a change in the AES Si–C peak ratios is not observed. On the other hand, the change in peak shape may alter the absolute peak-to-peak amplitudes and consequently impair their comparability. In addition, the superstructure disappears rapidly, not caused by electron beam damage but probably by residual gas contamination. Therefore, a determination of surface stoichiometry by AES alone seems ambiguous.

The poor stability of the new structure did not allow the acquisition of a complete $I(E)$-data set, especially superstructure spots were too weak. In addition, at low energies (cf., Fig. 9a) a diffuse background is visible with enhanced intensities around the (1/2,0) position indicating some degree of disorder on the surface. Further experimental efforts will be necessary to solve this problem. However, it was possible to monitor the (10)-spectrum after different annealing temperatures. In Fig. 9c this is shown for a fresh sample immediately after introduction into vacuum and for the same sample after a brief and a prolonged annealing to 1160 K. A structural change is visible in the low-energy region after a short thermal treatment. Although the long annealing step is necessary to obtain the new $(\sqrt{3} \times \sqrt{3})$R30° periodicity the structure of the $I(E)$-spectrum remains the same. This experiment depicts the local surface structure, with oxygen depletion and carbon–carbon bonds being present already after the brief annealing step. The extended thermal treatment is only responsible for the long-range periodicity of this new structure.

4. Conclusion

The preparation of SiC samples oriented along the (0001) plane by ex-situ oxidation and HF etching leads to atomically flat surfaces on a 1000 Å scale with well-developed bulk-like periodicity and stoichiometry. This was shown for the example of 6H-SiC(0001) samples immediately after introduction into UHV without further treatment. The oxidation step turned out to be essential to achieve this situation. It was possible to demonstrate a relation of the step morphology and the periodicity normal to the surface by STM. Obviously, the preparation procedure predominantly uncovered one of three inequivalent layers present in a 6H-sample. However, further experimental effort is necessary to improve the reproducibility of the preparation as depicted by experimental LEED $I(E)$ measurements on different samples and confirmed by a separate structure determination [5]. The surface dangling bonds of the chemically prepared surface are terminated by hydroxyl groups which are sensitive to electron irradiation. Thermal treatment removes the remaining oxygen from the surface and eventually leads to the development of a new $(\sqrt{3} \times \sqrt{3})$R30° superstructure where carbon–carbon bonds are present on the surface.

Acknowledgements

This work was supported by Deutsche Forschungsgemeinschaft (DFG) through Sonderforschungsbereich 292. U.S. is grateful to DFG for additional financial support.

References

[1] G. Pensl and R. Helbig, Silicon Carbide (SiC) – Recent Results in Physics and in Technology, in: Festkörperprobleme/Advances in Solid State Physics, Vol. 30, Ed. U. Rössler (Vieweg, Braunschweig, 1990) p. 133.

[2] J.W. Palmour, H.S. Kong and R.F. Davis, Appl. Phys. Lett. 51 (1987) 2028.

[3] L. Hoffmann, G. Ziegler, D. Theis and C. Weyrich, J. Appl. Phys. 53 (1982) 6962.

[4] R. Verma and P. Krishna, Polymorphism and Polytypism in Crystals (Wiley, New York, 1966).

[5] J. Schardt, Ch. Bram, S. Müller, U. Starke, K. Heinz and K. Müller, Surf. Sci., in press.

[6] W.J. Choyke, Optical and Electronic Properties of SiC, in: The Physics and Chemistry of Carbides, Nitrides and Borides, Ed. R. Freer (NATO ASI Series, Manchester, 1989).

[7] E.G. Acheson, Brit. Pat. 17 (1892) 911.

[8] J.A. Lely, Ber. Dtsch. Keram. Ges. 32 (1955) 229.

[9] Y.M. Tairov and V.F. Tsetkov, J. Cryst. Growth 52 (1981) 146.

[10] J.A. Powell, L.G. Matus and M.A. Kuczmarski, J. Electrochem. Soc. 134 (1987) 1558.

[11] J.A. Powell, L.G. Matus, M.A. Kuczmarski, C.M. Chorey, T.T. Cheng and P. Pirouz, Appl. Phys. Lett. 51 (1987) 823.

[12] T.T. Cheng, P. Pirouz and J.A. Powell, Mater. Res. Soc. Proc. 148 (1989) 229.

[13] J.A. Powell, D.J. Larkin, L.G. Matus, W.J. Choyke, J.L. Bradshaw, L. Henderson, M. Yoganathan, J. Yang and P. Pirouz, Appl. Phys. Lett. 56 (1990) 1353.

[14] H.S. Kong, J.T. Glass and R.F. Davis, J. Appl. Phys. 64 (1988) 2672.

[15] H. Matsunami, T. Ueda and H. Nashino, Mater. Res. Soc. Proc. 162 (1990) 397.

[16] J.A. Powell, J.B. Petit, J.H. Edgar, I.G. Jenkins, L.G. Matus, J.W. Yang, P. Pirouz, J.W. Choyke, L. Clemen and M. Yoganathan, Appl. Phys. Lett. 59 (1991) 183.

[17] A.J. van Bommel, J.E. Crombeen and A. van Tooren, Surf. Sci. 48 (1975) 463.

[18] F. Bozso, L. Muehlhoff, M. Trenary, W.J. Choyke and J.T. Yates, Jr., J. Vac. Sci. Technol. A 2 (1984) 1271.

[19] S. Adachi, M. Mohri and T. Yamashina, Surf. Sci. 161 (1985) 479.

[20] V.M. Bermudez, T.M. Parrill and R. Kaplan, Surf. Sci. 173 (1986) 234.

[21] R. Kaplan and T.M. Parrill, Surf. Sci. 165 (1986) L45.

[22] R. Kaplan, J. Vac. Sci. Technol. A 6 (1988) 829.

[23] L. Muehlhoff, M.J. Bozack, W.J. Choyke and J.T. Yates, J. Appl. Phys. 60 (1986) 2558.

[24] L. Muehlhoff, W.J. Choyke, M.J. Bozack and J.T. Yates, J. Appl. Phys. 60 (1986) 2842.

[25] R. Kaplan, Surf. Sci. 215 (1989) 111.

[26] S. Nakanishi, H. Tokutaka, S. Nishimori, S. Kishida and N. Ishihara, Appl. Surf. Sci. 41/42 (1989) 44.

[27] J.M. Powers and G.A. Somorjai, Surf. Sci. 244 (1991) 39.

[28] C.-S. Chang, N.-J. Zheng, I.S.T. Tsong, Y.-C. Cheng and R.F. Davis, J. Am. Ceram. Soc. 73 (1990) 3264.

[29] C.-S. Chang, I.S.T. Tsong, Y.C. Wang and R.F. Davis, Surf. Sci. 256 (1991) 354.

[30] P. Heuell, M.A. Kulakov, V.F. Tsvetkov and B. Bullemer, Proc. Int. Conf. on Silicon Carbide and Related Materials, Washington, 1994, submitted.

[31] S. Karmann, W. Suttrop, A. Schöner, M. Schadt, C. Haberstroh, F. Engelbrecht, R. Helbig and G. Pensl, J. Appl. Phys. 72 (1992) 5437.

[32] K. Besocke, Surf. Sci. 181 (1987) 145.

[33] J.J. Bellina, Jr. and M.V. Zeller, Appl. Surf. Sci. 25 (1986) 380.

[34] M. Dayan, J. Vac. Sci. Technol. A 4 (1986) 38.

[35] B. Jorgensen and P. Morgen, J. Vac. Sci. Technol. A 4 (1986) 1701.

[36] B. Jorgensen and P. Morgen, Surf. Interf. Anal. 16 (1990) 199.

[37] R. Fuchs and K.L. Kliewer, Phys. Rev. A 140 (1965) 2076.

[38] H. Ibach, H. Wagner and D. Bruchmann, Solid State Commun. 42 (1982) 457.

[39] P.-R. Steiner, L. Hammer, U. Starke and K. Müller, in preparation.

[40] H. Ibach and D.L. Mills, Electron Energy Loss Spectroscopy and Surface Vibrations (Academic Press, New York, 1982).